Protostellar accretion in low mass metal poor stars and the cosmological lithium problem
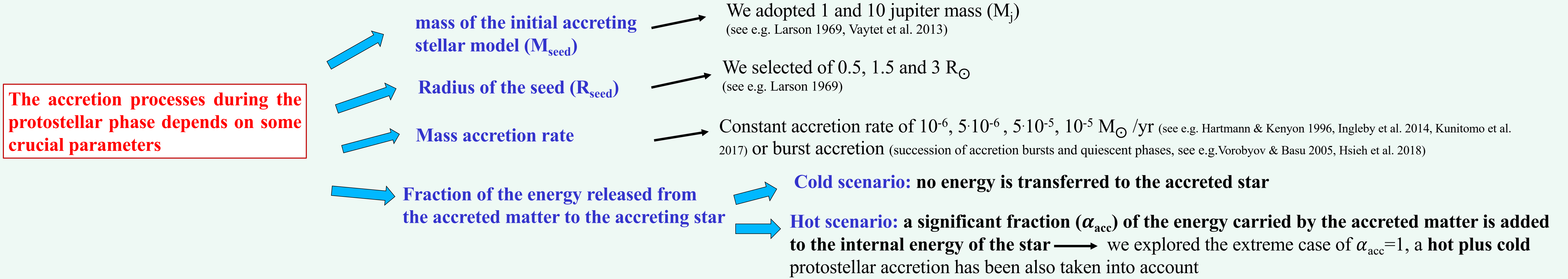
scilla.deglinnocenti@unipi.it

E. Tognelli[1], P.G. Prada Moroni[1,2], S. Degl'Innocenti[1,2], M. Salaris[3], S. Cassisi[4]

[1] Dipartimento di Fisica "E.Fermi" Università di Pisa, Italy   [2] INFN – Sezione di Pisa, Italy   [3] Astrophysics Research Institute, John Moores University, U.K.   [4] INAF- Osservatorio Astronomico d'Abruzzo, Italy

Metal-poor, field dwarf stars with effective temperature larger than about 5900 K and $-3 \lesssim$ [Fe/H] $\lesssim -1.5$ show a quite uniform surface Li abundance (the so called "Spite Plateau") which, following canonical models of stellar evolution and Galactic chemical enrichment, should be equivalent to the primordial Li abundance. A significant disagreement with the predictions of the Big Bang Nucleosynthesis is however present (see e.g. Meléndez et al. 2010 and references therein). A possible astrophysical solution involves lithium burning due to protostellar mass accretion on Spite plateau stars. To date, the initial accretion from a circumstellar disc onto a central seed in low mass stars has mainly been modelled at solar metallicity (see e.g. Baraffe et al. 2009, 2012; Hartmann et al. 2016, Kunitomo et al. 2017, 2018). We thus explored the possible impact on the Pre-Main Sequence/Main Sequence (PMS/MS) Li abundances of the accretion phase during the protostellar evolution in the metal-poor regime.

1 - THE EVOLUTIONARY FRAMEWORK

We computed the detailed evolution from the protostellar stage up to the MS of models with final masses equal to 0.7 and 0.8 $M_\odot$, for metallicity equal to [Fe/H] = -2.1, -1.1, typical of Spite plateau stars. The stellar models were computed with the Pisa version of the FRANEC evolutionary code (Degl'Innocenti et al. 2008; Dell'Omodarme et al. 2012), adopting the same input physics and parameters together with the same treatment for protostellar mass accretion described in Tognelli et al. (2015, 2018). For more details see Tognelli et al. 2020.

The accretion processes during the protostellar phase depends on some crucial parameters

→ **mass of the initial accreting stellar model (M_{seed})** → We adopted 1 and 10 jupiter mass (M_J) (see e.g. Larson 1969, Vaytet et al. 2013)

→ **Radius of the seed (R_{seed})** → We selected of 0.5, 1.5 and 3 $R_\odot$ (see e.g. Larson 1969)

→ **Mass accretion rate** → Constant accretion rate of 10^{-6}, $5 \cdot 10^{-6}$, $5 \cdot 10^{-5}$, 10^{-5} $M_\odot$ /yr (see e.g. Hartmann & Kenyon 1996, Ingleby et al. 2014, Kunitomo et al. 2017) or burst accretion (succession of accretion bursts and quiescent phases, see e.g.Vorobyov & Basu 2005, Hsieh et al. 2018)

→ **Fraction of the energy released from the accreted matter to the accreting star**

→ **Cold scenario:** no energy is transferred to the accreted star

→ **Hot scenario:** a significant fraction (α_{acc}) of the energy carried by the accreted matter is added to the internal energy of the star → we explored the extreme case of α_{acc}=1, a **hot plus cold** protostellar accretion has been also taken into account

2 – COLD ACCRETION MODELS

Dependence on R_{seed}

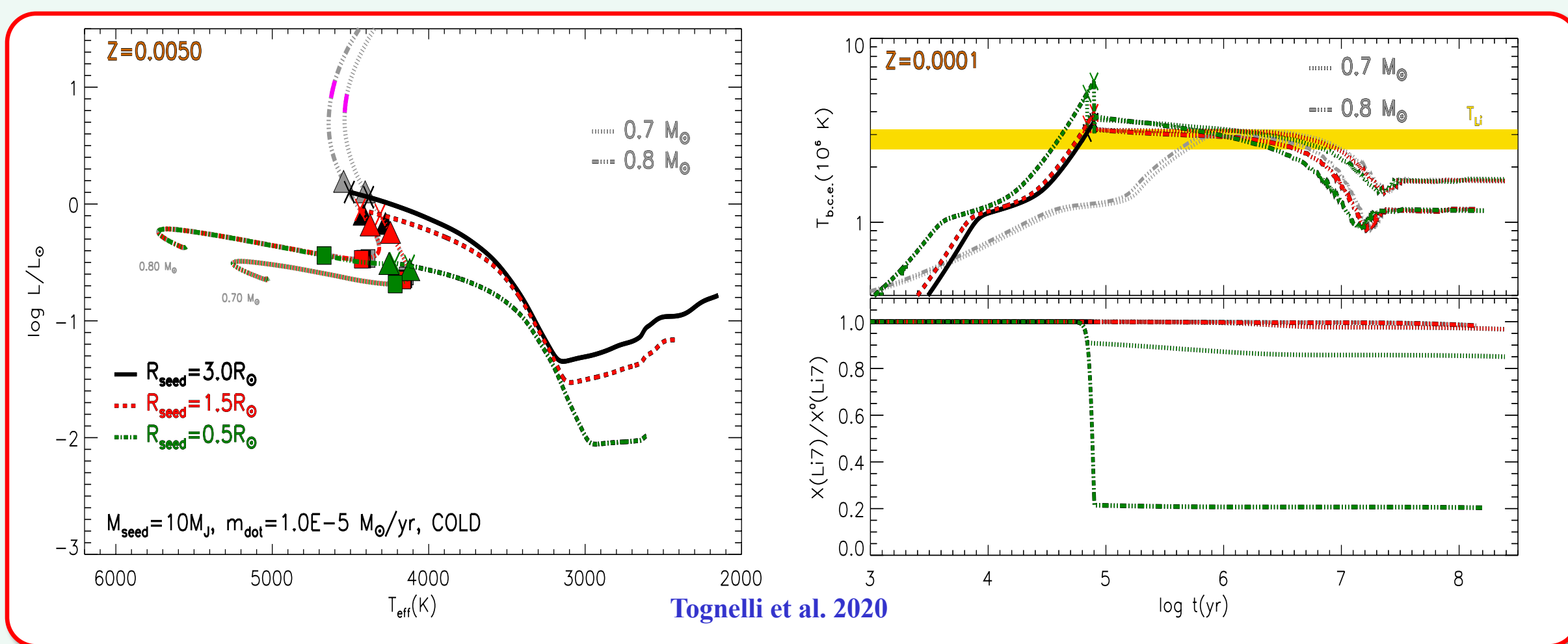**Fig. 1** Accreting models with $Z = 0.0001$, final masses of M_{fin}=0.7 and 0.8 $M_\odot$, $\dot{m} = 10^{-5}$ $M_\odot$ yr^{-1}, M_{seed}=10 M_J, and R_{seed}=0.5, 1.5, and 3.0 $R_\odot$. Standard non-accreting models are also shown (grey lines). *Left panel:* HR diagram. The position of models at 1 Myr (filled triangles) and 10 Myr (filled squares), the region corresponding to the deuterium burning phase (thick magenta line), and the end of the accretion phase (crosses) are marked. *Right panel:* time evolution of the temperature at the bottom of the convective envelope and surface Li abundance (divided by the initial one) for the accreting and non-accreting models (the latter are shown with grey lines). The horizontal yellow shaded region denotes the Li burning temperature range.
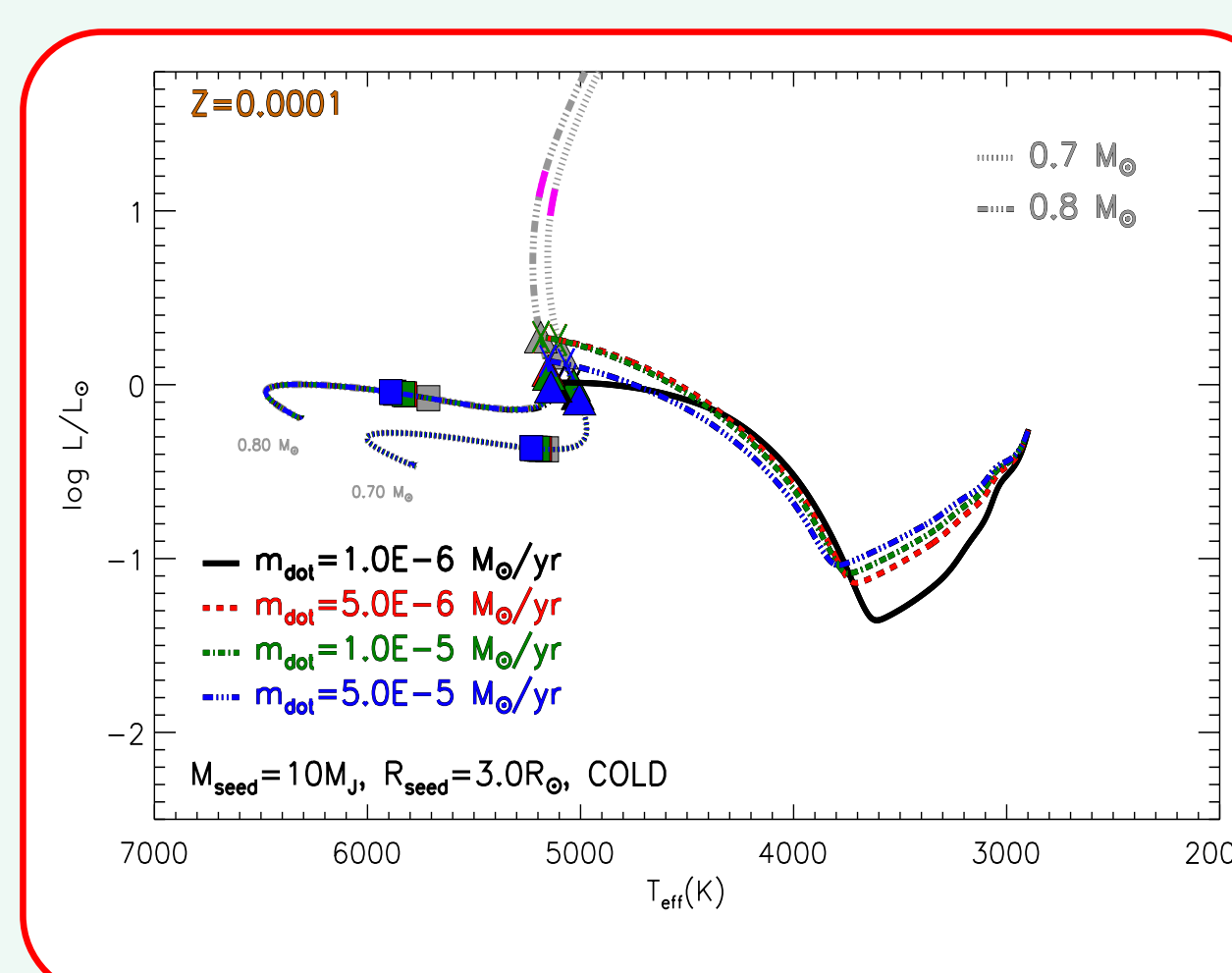
Dependence on $\dot{m}$

Fig. 2 HR diagram of accreting models with Z=0.0001, M_{seed}=10 M_J, R_{seed}=3.0 $R_\odot$ and final masses M_{fin} = 0.7 and 0.8 $M_\odot$, for different accretion rates, $\dot{m}$ = 10^{-6}, $5 \cdot 10^{-6}$, 10^{-5}, $5 \cdot 10^{-5}$ $M_\odot$ yr^{-1}. The symbols are the same as in Fig.1.

The general evolution during the accreting phase is not significantly affected by the exact value of $\dot{m}$

Dependence on M_{seed}
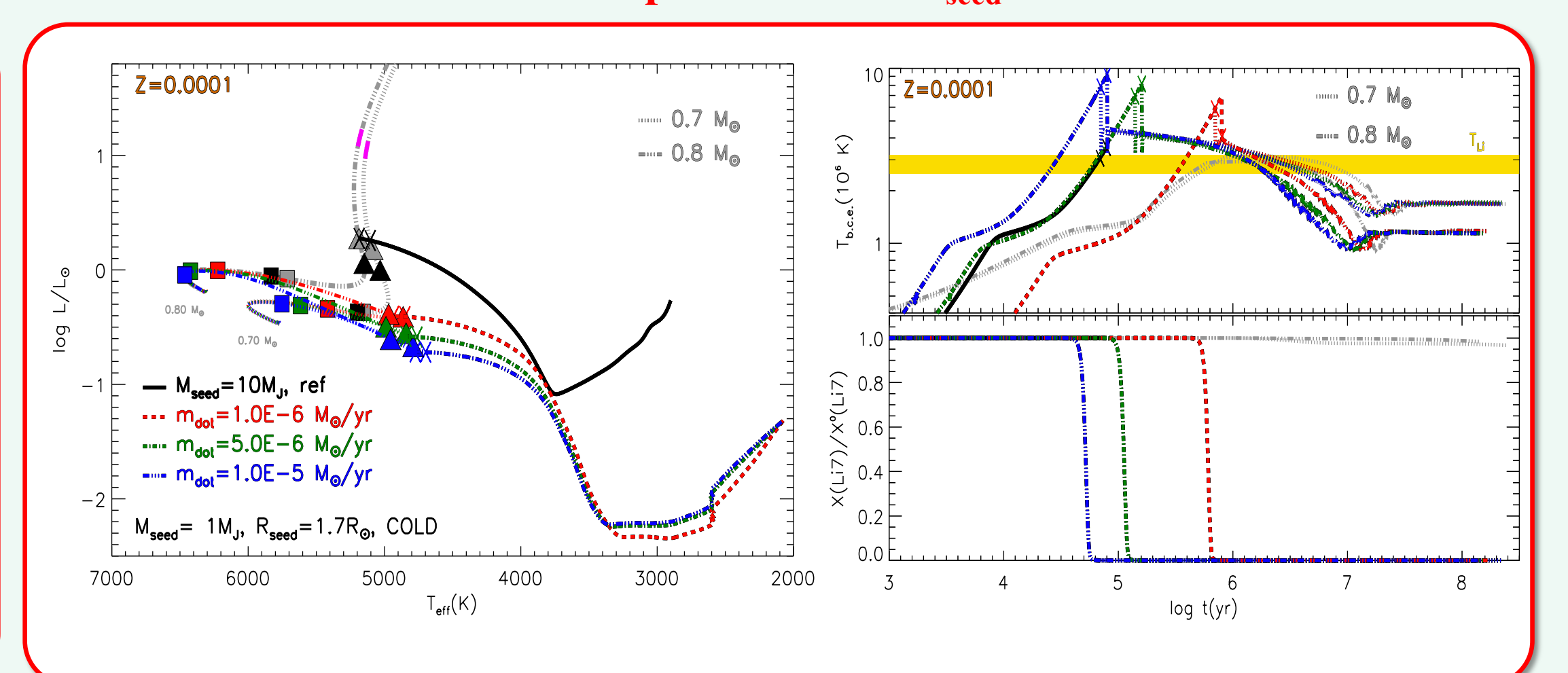
Fig. 3 As in Fig.2 but for M_{seed}=1 M_J. The "reference" model (with M_{seed}=10 M_J and $\dot{m}$ = 10^{-5} yr^{-1}) is also shown in black. *Left panel:* HR diagram. *Right panel:* time evolution of the temperature at the bottom of the convective envelope and surface Li abundance (divided by the initial one) for the accreting and non-accreting models (the latter are shown with grey lines).

Dependence on M_{seed} and R_{seed}

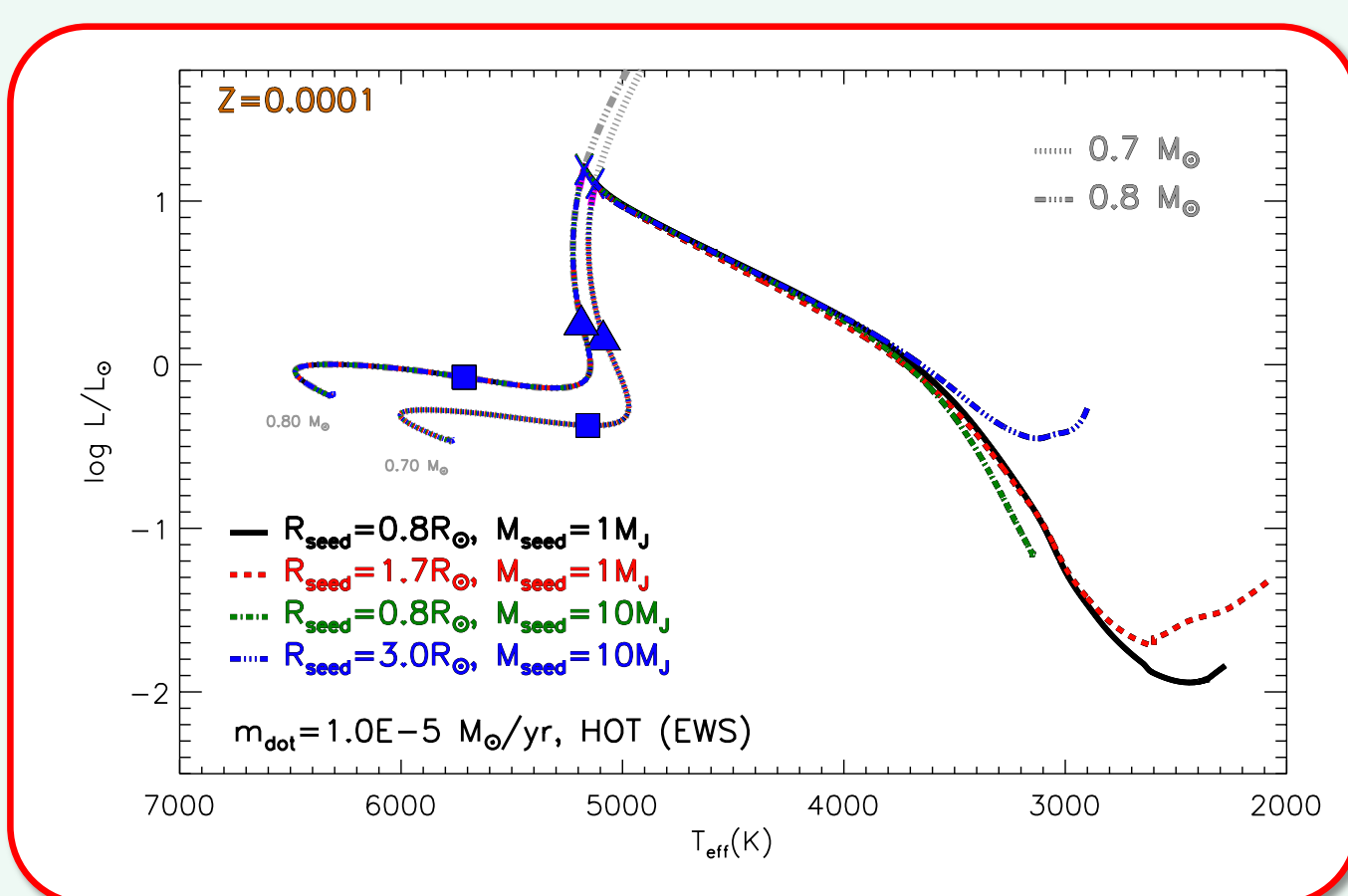**Fig. 4** Evolution in the HR diagram of hot accreting models, final masses of M_{fin}=0.7 and 0.8 $M_\odot$, with different values of R_{seed} and M_{seed}. The standard non-accreting model (grey lines) is also shown. The position of models at 1 Myr (filled triangles) and 10 Myr (filled squares), deuterium burning region (thick magenta line), and the end of the accretion phase (cross) are marked.
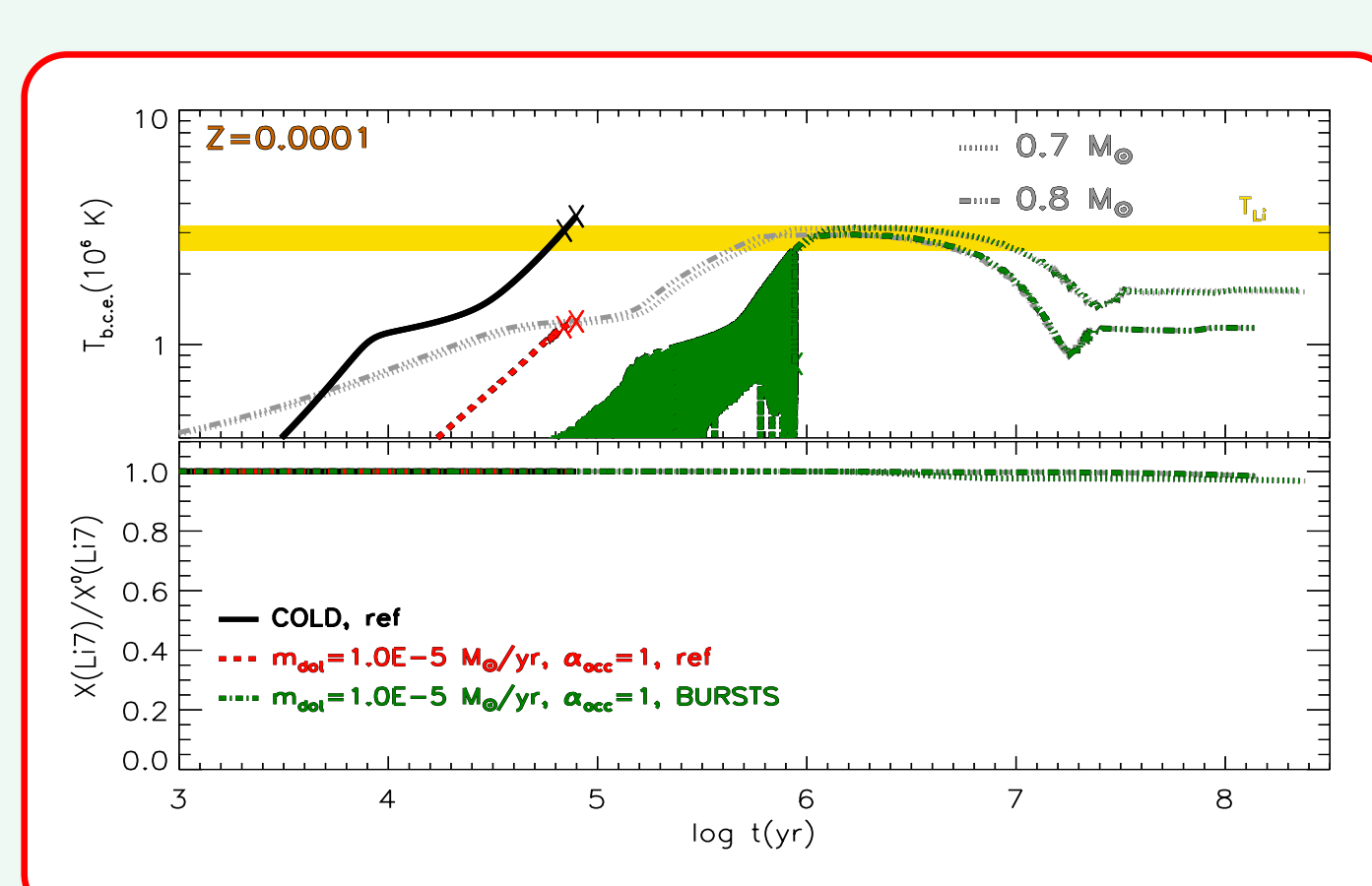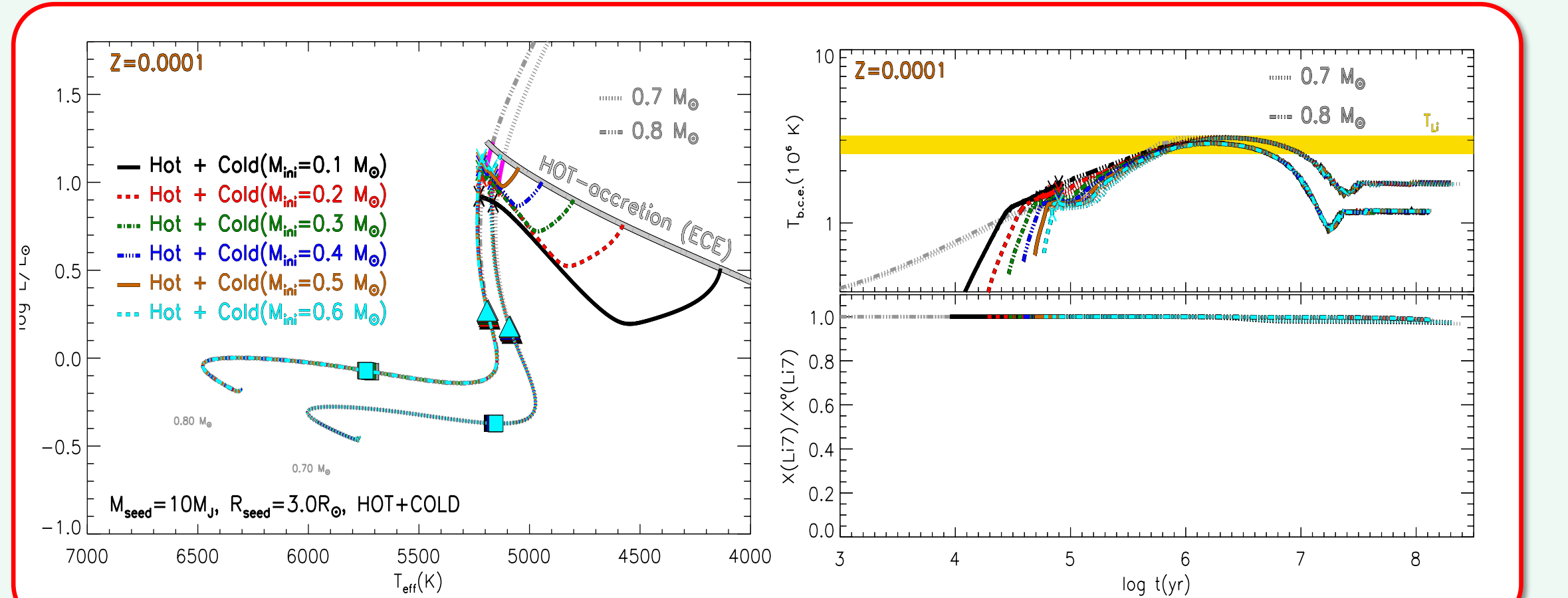
Burst accretion

Fig. 5 Temporal evolution of the temperature at the bottom of the convective envelope and surface lithium abundance (divided by the initial value). The values are shown for the hot bursts accreting models with Z = 0.0001, final masses of M_{fin}=0.7 and 0.8 $M_\odot$ (green line), standard non-accreting models (grey line), reference cold accreting models (black line) and reference hot accreting models (red line)

3 – HOT ACCRETION MODELS

Fig. 6 Evolution of hot plus cold accretion models with Z=0.0001, final masses of M_{fin}=0.7 and 0.8$M_\odot$, M_{seed}=10 M_J, R_{seed}=3$R_\odot$, and $\dot{m}$ =10^{-5} $M_\odot$ yr^{-1}. The results are shown for different mass values (M_{ini}) at the beginning of the cold disc accretion. Standard non-accreting models (grey lines) are also shown. *Left Panel:* HR diagram, symbols as in Fig. 4. The position of the beginning of the cold disc accretion for different starting masses is also shown. *Right panel:* temporal evolution of the temperature at the bottom of the convective envelope and surface lithium abundance (normalised to the initial one).

Hot plus cold protostellar accretion

Hot accretion (for both constant and burst accretion) and hot plus cold accretion do not produce relevant effects on the stellar structure.
The PMS Li evolution is the same as in standard non-accreting models

4 – RESULTS

Whenever the accretion process produces bright and extended configurations during the protostellar stage, the resulting structure at the end of the accretion closely resembles, for both the structural properties and the surface Li abundance, a standard, non-accreting star with the same final mass.

For the hot and hot plus cold protostellar accretion case models are expanded and bright → **Regardless of the exact choice about the seed mass and radius the models and the surface Li abundance are barely affected by the accretion process.**

For cold protostellar accretion, the PMS evolution and the surface lithium abundance are largely affected when adopting small values for M_{seed} and R_{seed} →

- **PMS models do not follow the standard Hayashi track and a significant Li depletion can be obtained**
- **The results depend strongly on the initial conditions and on the final stellar mass**

This is due to the impact that the various assumptions about the initial conditions (M_{seed} and R_{seed}) have on the Kelvin-Helmholtz timescale (τ_{KH}), and how τ_{KH} compares with the accretion time ($\tau_{acc} \propto 1/\dot{m}$)

→ if $\tau_{KH} < \tau_{acc}$ the PMS evolution is driven by the surface radiative losses, the impact of the accretion process is negligible (see also e.g. Baraffe et al. 2009, 2012; Baraffe & Chabrier 2010 for disk star calculations)

→ if $\tau_{KH} > \tau_{acc}$ (small M_{seed} and R_{seed}) the evolution is mainly governed by the accretion process

5 – CONCLUSIONS

A significant reduction of the surface lithium abundance can be obtained only for a restricted range of accretion parameters. The corresponding models show an evolution in the HR diagram that is quite different from the one observed for high metallicity PMS stars. A fine tuning of the protostellar accretion parameters is required to reproduce, starting from BBN abundances, the observed constant abundance for the mass and metallicity ranges typical of the Spite plateau.

References

Baraffe I. et al. 2009, ApJ, 702, L27
Baraffe I. & Chabrier G. 2010, A&A, 521, A44
Baraffe I. et al. 2012, ApJ, 756, 118

Degl'Innocenti S. et al. 2008, Ap&SS, 316, 25
Dell'Omodarme M. et al. 2012, A&A, 540, A26
Hartmann L. et al. 2016, ARA&A, 54, 135
Hartmann L. & Kenyon S.J. 1996, ARA&A, 34, 207

Hsieh T.H. et al. 2018, ApJ, 854, 15
Kunimoto M. et al. 2017, A&A, 599, A49
Kunimoto M. et al. 2018, A&A, 618, A132

Ingleby L. et al. 2014, ApJ, 790, 47
Larson R. B. 1969, MNRAS, 145, 271
Meléndez J. et al. 2010, A&A, 515, L3

Tognelli E. et al. 2015, MNRAS, 454, 4037
Tognelli E. et al. 2018, MNRAS, 476, 27
Tognelli E. et al. 2020, A&A, 638, A81

Vaytet N. et al. 2103, A&A, 557, A90
Vorobyov E.I. & Basu S. 2005, ApJ, 633, L137